Numerical simulations of self-propagating eddies collision with obstacles

Tiago Carrilho Biló
C# 11950866
tcb46@miami.edu

Rosenstiel School of Marine and Atmospheric Science - Computer Models in Fluid Dynamics (MPO 762) - Project Report

December 12, 2016

1 Introduction

Oceanic rings and vortices have an important role in the global-scale circulation by transporting and modifying properties throughout the oceans (e. g., *Talley et al.*, 2011). Since observations are sparse in space and time, numerical and physical models consist an important framework to understand the behavior and dynamics of such important features (e. g., *Cenedese et al.*, 2005; *Early et al.*, 2011). Therefore, motivated by this I decided to study the behavior of self-propagating eddies collision with obstacles in a series of idealized numerical experiments as part of the Computer Models in Fluid Dynamics (MPO 762) coursework project. In sections 2 and 3, I describe the numerical experiments set-up and the results respectively.

2 The model

In this work the self-propagating eddies were studied using an unforced, inviscid, reduced-gravity model in the β-plane described by Equations 1, 2 and 3:

$$\frac{du}{dt} + fv = -g\frac{\partial \eta}{\partial x}, \tag{1}$$

$$\frac{dv}{dt} - fu = -g\frac{\partial \eta}{\partial y}, \tag{2}$$

$$\frac{\partial \eta}{\partial t} + \frac{\partial hu}{\partial x} + \frac{\partial hv}{\partial y} = 0, \tag{3}$$

where (x,y) are the spatial coordinates, t is the time, (u,v) are the velocity components, η is the displacement of the interface between the active and motionless layer, $\frac{d}{dt} = \frac{\partial}{\partial t} + u\frac{\partial}{\partial x} + v\frac{\partial}{\partial y}$ is the total time derivative operator, $f = f_0 + \beta y$ is planetary vorticity, g is the reduced gravity term, and $h = H + \eta$ is the thickness of the active layer.

The system of equations shown above was discretized on an Arakawa C-grid and manipulated in order to enforce mechanic energy conservation following Equations 4, 5 and 6. Then the system was integrated using a RK3 time stepping scheme.

$$\frac{\partial u_{i\pm\frac{1}{2},j}}{\partial t} - \overline{q\overline{V}^{x}}^{y} + \delta_x \Phi_{i\pm\frac{1}{2},j} = 0, \tag{4}$$

$$\frac{\partial v_{i,j\pm\frac{1}{2}}}{\partial t} + \overline{q\overline{U}^{y}}^{x} + \delta_y \Phi_{i,j\pm\frac{1}{2}} = 0, \tag{5}$$

$$\frac{\partial \eta_{i,j}}{\partial t} + \delta_x U_{i,j} + \delta_y V_{i,j} = 0, \tag{6}$$

where (i,j) are the grid ells indexes, (δ_x, δ_y) are the centered difference partial derivatives in x and y, $U_{i\pm\frac{1}{2},j} = \overline{h}^{x}_{i\pm\frac{1}{2},j} \times u_{i\pm\frac{1}{2},j}$ is the mass flux through the x-face of the grid cell, $V_{i,j\pm\frac{1}{2}} = \overline{h}^{y}_{i,j\pm\frac{1}{2}} \times v_{i,j\pm\frac{1}{2}}$ is the mass flux through the y-face of the grid cell, $\Phi_{i,j} = g\eta_{i,j} + \frac{\overline{u^2}^{x} + \overline{v^2}^{y}}{2}$ is called the total head, $q_{i\pm\frac{1}{2},j\pm\frac{1}{2}} = \frac{\delta_x v - \delta_y u + f}{\overline{h}^{xy}}$ is the potential vorticity term, and the over bars represent the average operation along an axis.

2.1 Model set-up

All the numerical solutions were evaluated in a rectangular domain with closed boundaries (i. e., no normal flow and fluxes to the boundaries), centered at $(x,y) = 0$ km, and area of $L_x \times L_y$. The parameters required to integrate the Equations 4, 5 and 6 were chosen accordantly with the general characteristics of

the North Brazil Current (NBC) Rings at the region where it encounter the Lesser Antilles (e. g., *Fratantoni and Richardson*, 2006) [Table 3]. Since the NBC rings have high propagation speeds and large dimensions, I could choose proper resolution and time step that made my code efficient and stable (see Table 3).

Table 1: Specific model parameters, spatial resolution, time step and domain dimensions used in this study.

g	f_0	β	**H**	Δx	Δy	L_x	L_y	Δt
$4.5\times10^{-3}\ \frac{m}{s^2}$	$3.3\times10^{-5}\ \frac{1}{s}$	$2\times10^{-11}\ \frac{1}{ms}$	1000 m	2 km	2 km	1500 km	600 km	15 min

The experiments initialization was performed in a similar way (see Table 2) and integrated over 60 days. The initial condition consist of a symmetric geostrophic anticyclonic eddy with approximately 200 km of diameter, maximum velocities of approximately 1 m s^{-1}, and placed on the eastern "hemisphere" of the domain. The eddy structure defined by equations 7, 8, and 9 was based on *Dengler et al.* (2004) parametric model for the Deep Western Boundary Current Eddies at 8°S-18°S.

$$v(x,y,t=0) = -s\frac{U(x-x_0)e^{\phi}e^{\gamma}}{Rd}, \tag{7}$$

$$u(x,y,t=0) = s\frac{U(y-y_0)e^{\phi}e^{\gamma}}{Rd}, \tag{8}$$

$$\eta(x,y,t=0) = s\frac{Uf_0Rde^{\phi}e^{\gamma}}{2g}, \tag{9}$$

where (x_0, y_0) are the coordinates of the eddy center, U is the double of the maximum velocity, $s = \frac{f_0}{|f_0|}$ is the hemisphere factor, $\phi = -\frac{(x-x_0)^2}{Rd^2}$ is the zonal structure, $\gamma = -\frac{(y-y_0)^2}{Rd^2}$ is the meridional structure, and $Rd = \frac{\sqrt{gH}}{|f_0|}$ is the Rossby deformation radius.

Table 2: Initial condition parameters used in all numerical experiments.

x_0	y_0	**Rd**	**U**
-300 km	0 km	~70 km	$2\ \frac{m}{s}$

2.2 Experiments

In this study I performed a set of 8 numerical experiments divided in two groups. The first group consists of two "diagnostic" experiments where the anticyclonic eddies were allowed to self-propagate without colliding with obstacles (experiments **nt-hn** and **nt-hs**). The purpose of such configuration is to guarantee that there is no bug in the code and to verify for how long the eddies can keep the velocity structure. The difference between these experiments is the earth's hemisphere where the eddies are propagating (i. e., sign of f).

The second group of numerical simulations is formed by experiments with different configurations of a set of circular obstacles (or islands) placed at the center of the domain (i. e., $x = 0$). The islands radius (r) are approximately 40 km and the distance between them are $5r$, $4r$, $2r$, r, $\frac{r}{2}$, and $\frac{r}{4}$ (Figure 1).

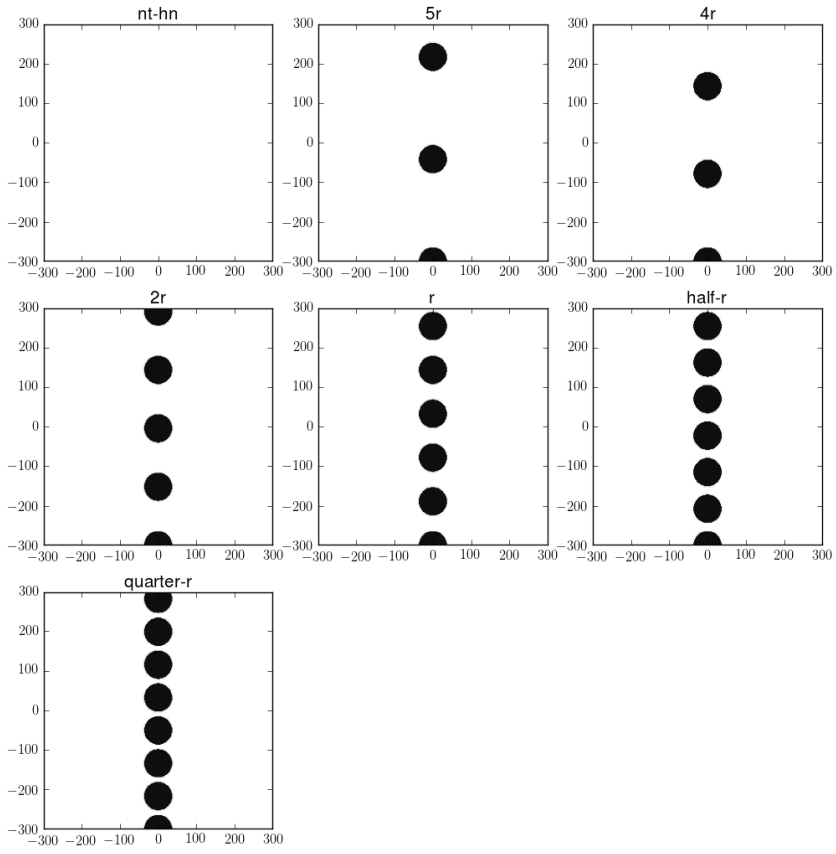

Figure 1: Obstacles (black circles), or meridional ridge, place at the center of the domain in each numerical experiment.

Table 3: Experiments list

	sign of **f**	**r (km)**	**distance between islands (km)**
nt-hn	+		
nt-hs	-		
5r	-	40	200
4r	-	40	160
2r	-	40	80
r	-	40	40
half-r	-	40	20
quarter-r	-	40	10

3 Results

3.1 Diagnostic

As mentioned before, in order to verify the numerical code the simulations **nt-hn** and **nt-hs** were initialized without obstacles. The eddies kept its velocity structure almost intact for 60 days with a prominent and closed relative vorticity minimum (maximum) center in experiment **nt-hn** (**nt-hs**). The location of these vorticity centers were tracked at each time step and plotted in order to observe the trajectories of the eddies. As expected, anticyclonic eddies propagate westward with a path deflected towards the equator (Figure 2) indicating there is no bug in the code and the initial condition was properly built (e. g., *Chelton et al.*, 2007).

Once the eddies start propagating as the model is integrated forward in time, the perfect geostrophic balance in Equations 4 and 5 is perturbed and part of the energy in the eddy starts propagating through the domain as Rossby and gravity internal waves (e. g., *Early et al.*, 2011). This energy loss generates a slightly asymmetry in the eddies velocity structure (Figure 3).

Additionally, I also monitored the total mechanic energy, enstrophy and the volume of water vertically displaced at the interface at each time step in all experiments. With the intent to verify if those properties are conserved I computed the percentage of change with respect the initial conditions according to Equation 10 (see Figure 4). As expected, the discretization scheme and the closed boundaries guarantee the conservations of energy (maximum changes of -1.5%) and volume (changes $\sim 10^{-13}\%$), however enstrophy is not conserved after approximately 5 days the initial interaction (t$\sim$ 30 days) of the eddies with the obstacles (see next section).

$$Change(t) = 100 \times \frac{Property(t=0) - Property(t=t_i)}{Property(t=0)} \tag{10}$$

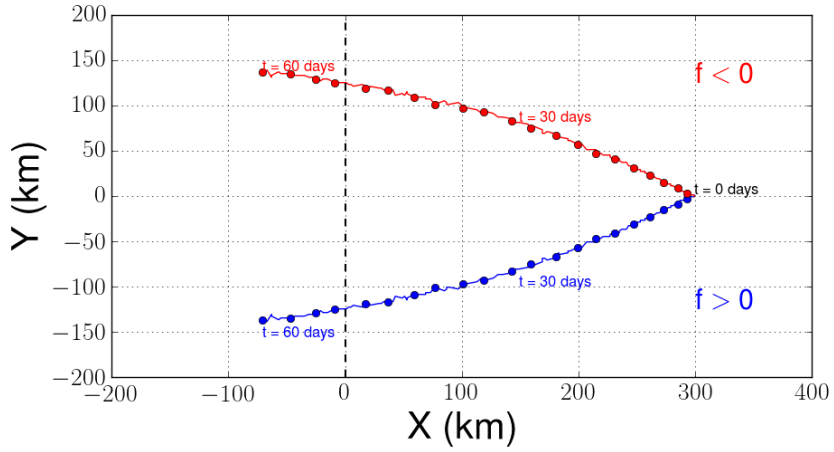

Figure 2: Location of the center of the eddy every 3 days in experiments **nt-hn** (blue dots) and **nt-hs** (red dots).

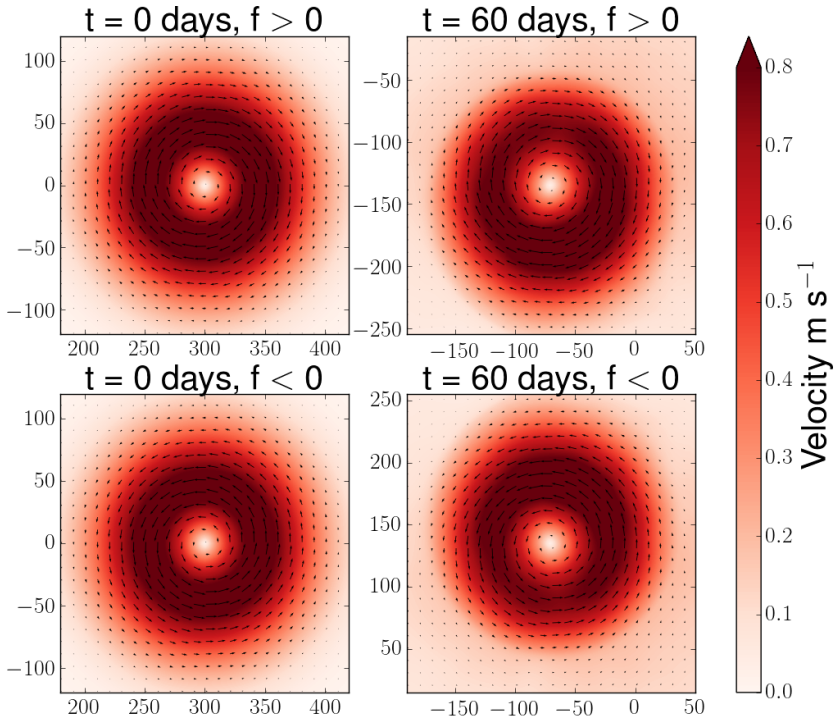

Figure 3: Velocity structure at t = 0 days (left panels) and t = 60 days (right panels) in experiments **nt-hn** (upper panels) and **nt-hs** (lower panels).

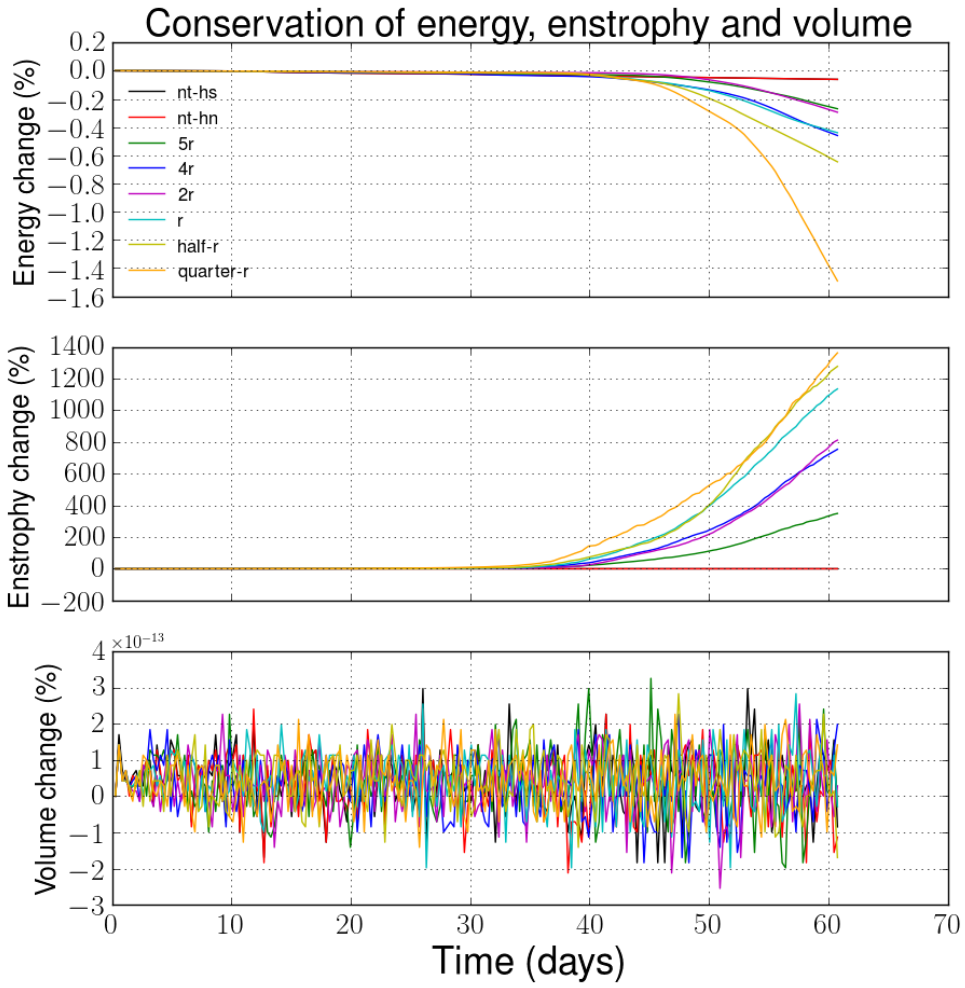

Figure 4: Percentage of change of the mechanic energy, enstrophy and displaced volume with respect to the initial conditions.

3.2 Eddy-behavior

In Figure 5 I present the velocity fields in experiments **nt-hn** and **4r** at different time steps. Note in both cases the eddy propagates southwestward, however at $t \sim$60 days the eddy starts interacting with one of the islands in **4r**. As this interaction evolves circulation around the obstacles and on the western part of the domain develop, and the well defined eddy-structure is destroyed. By the time the simulation ends there are no well organized currents, eddies or small scale water "swirls" in the velocity fields due to the inefficiency of this model in conserving enstrophy. In turbulent flows like this the vorticity conservation plays an important constraint, therefore this model is able to predict the early moments of the interaction. This behavior was observed in all numerical experiments.

Keeping that in mind, Figure 6 shows a closer look at the eddy-obstacles interaction in different experiments between day 35 and 50. As the distance between islands decreases the anticyclonic eddy tends to be destroyed in a faster rate, and organized zonal jets tend to form in the channels. Note that the velocity perturbations tend to be more concentrated in the collision site for experiments where the islands are further apart.

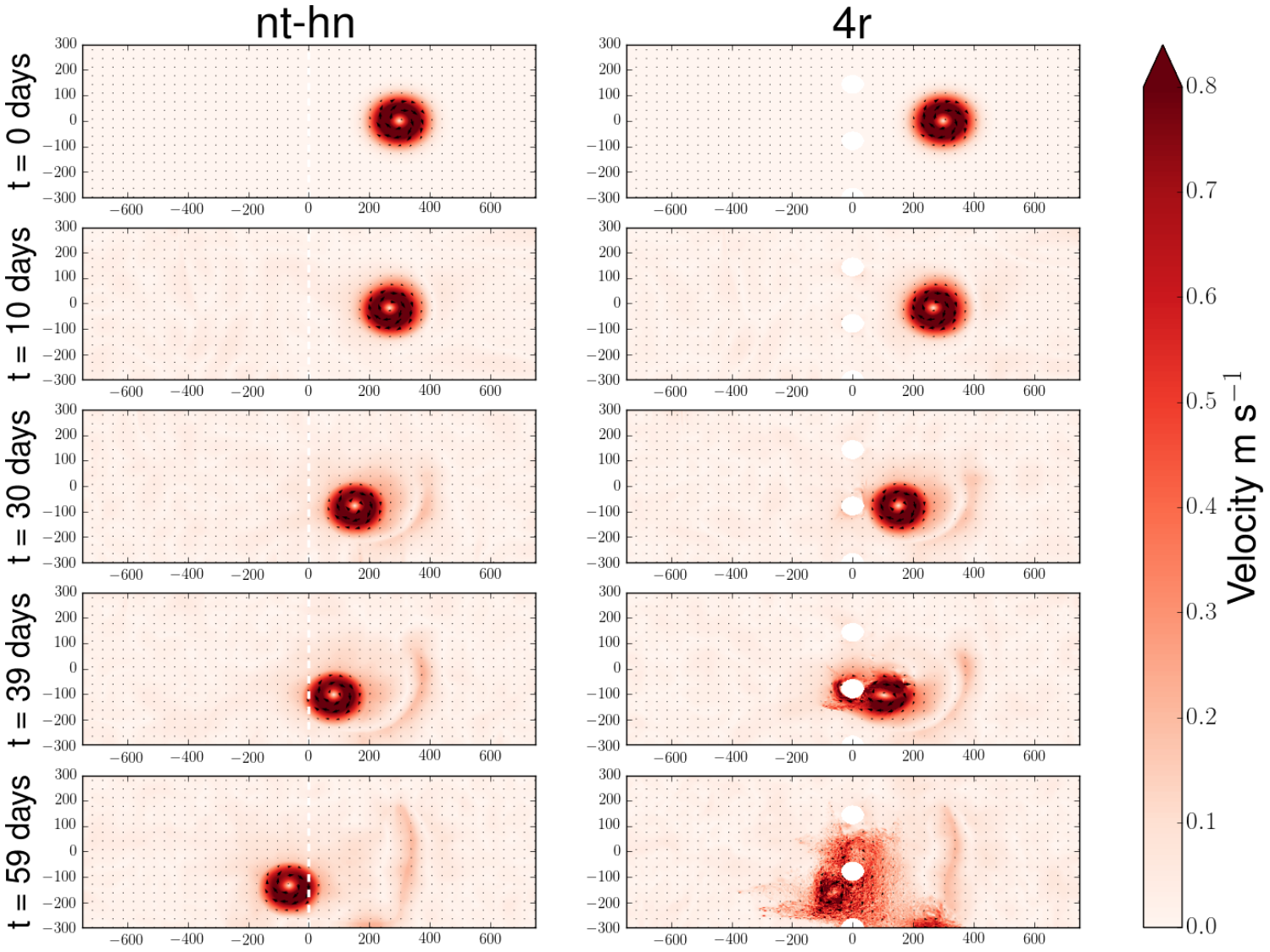

Figure 5: Velocity fields from experiments **nt-hn** (left panels) and **4r** (right panels).

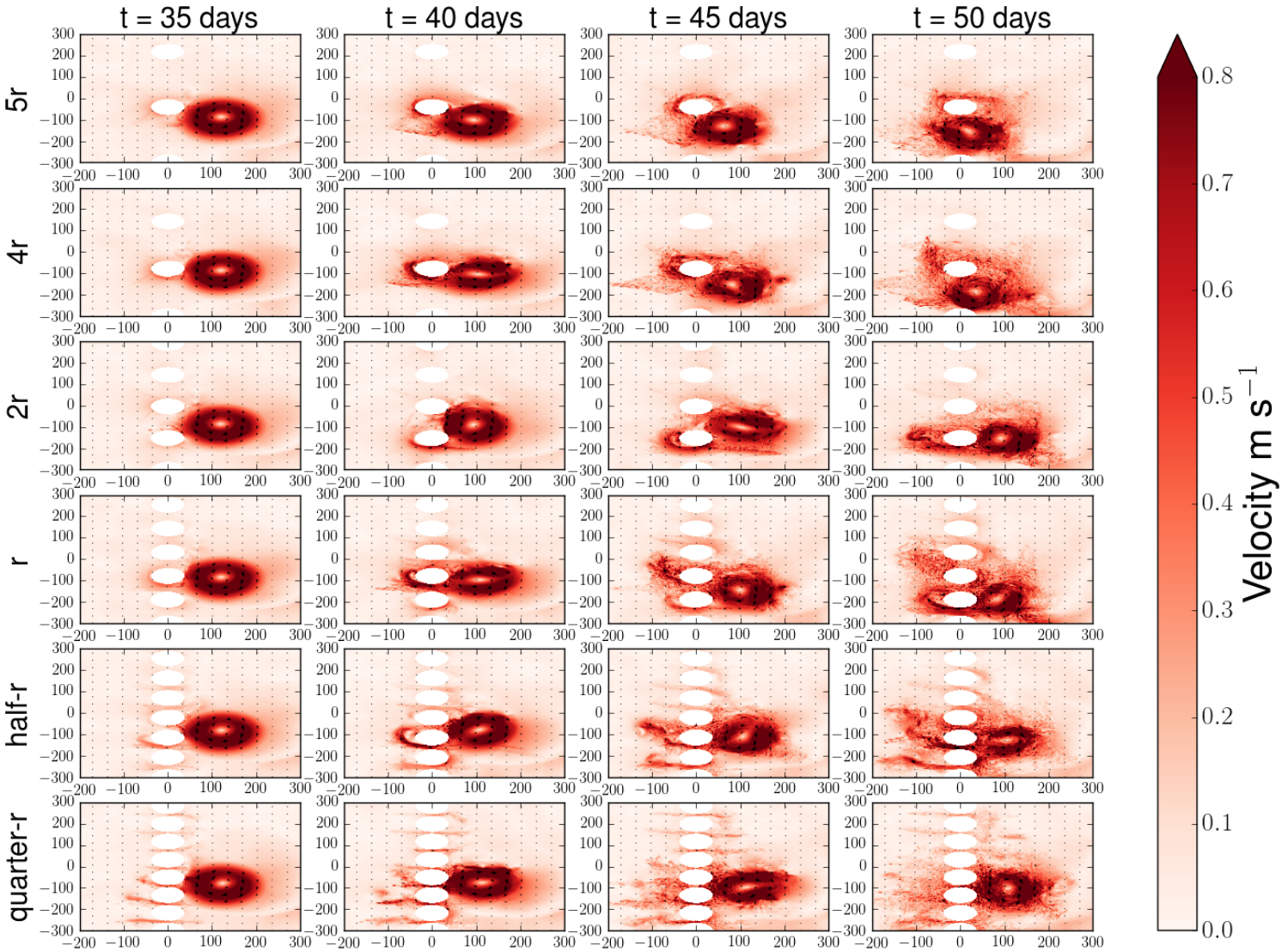

Figure 6: Velocity fields showing the collision of the eddy with the obstacles in all numerical experiments.

References

Cenedese, C., C. Adduce, and D. M. Fratantoni (2005), Laboratory experiments on mesoscale vortices interacting with two islands, *J. Geophys. Res.*, *110*(C9).

Chelton, D. B., M. G. S. R. M, Samelson, and R. A. Szoeke (2007), Global observations of large oceanic eddies, *34*(15).

Dengler, M., F. A. Schott, C. Eden, P. Brandt, J. Fischer, and R. J. Zantopp (2004), Break-up of the Atlantic deep western boundary current into eddies at 8°S, *Nature*, *432*(7020), 1018–1020.

Early, J. J., R. M. Samelson, and D. B. Chelton (2011), The evolution and propagation of quasigeostrophic ocean Eddies, *J. Phys. Oceanogr.*, *41*(8), 1535–1555.

Fratantoni, D. M., and P. L. Richardson (2006), The Evolution and Demise of North Brazil Current Rings, *J. Phys. Oceanogr.*, *36*(7), 1241–1264.

Talley, L. D., G. L. Pickard, W. J. Emery, and J. H. Swift (2011), *Descriptive Physical Oceanography: An Introduction*, sixth ed., Academic Press.